A Soft-Switched Parallel Inverter Architecture With Minimal Output Magnetics

David J. Perreault, John G. Kassakian, and Henrik Martin

Massachusetts Institute of Technology
Laboratory for Electromagnetic and Electronic Systems
Cambridge, MA 02139 USA

Abstract- **A parallel converter architecture based on the resonant pole topology is presented which minimizes the output magnetics required for current sharing. A novel current control scheme applicable to both the new parallel architecture and the single resonant pole inverter is described, and equations for piecewise modeling of the parallel architecture are presented. The paper demonstrates that the parallel architecture overcomes some of the major disadvantages of the conventional resonant pole inverter.**

INTRODUCTION

The construction of high power converter systems using paralleled low power converter cells has substantial potential advantages over conventional single large converter designs. These advantages include improved performance, reliability, and modularity, manufacturability, reduced cost, and the ability to switch at higher frequencies [1],[2]. While paralleled converter systems are often used at very high power levels [3-5], and in those applications which demand high reliability [6], the paralleled converters have not been of a size permitting mass production manufacturing techniques and high frequency switching.

To fully realize the benefits of a cellular architecture, converter topologies and control techniques suited to this architecture must be developed. In this paper we discuss some key issues in the design of cellular converter systems, and present a new parallel architecture implementation which addresses these design issues. This architecture eliminates some of the major drawbacks of the single resonant pole inverter (RPI), on which it is based. Furthermore, an enhanced control algorithm applicable to both single and parallel resonant pole inverters (PRPI) is presented which significantly reduces converter stresses and losses for many operating conditions. Finally, we describe a piecewise simulation model for the new architecture, and present examples and simulation results illustrating the benefits of the approach.

0-7803-1859-5/94/$4.00 © 1994 IEEE

CURRENT SHARING

The construction of a large converter by paralleling smaller converter cells requires that a current sharing mechanism be included to prevent the destructive overload of individual cells. Current sharing can be achieved by using an appropriate control scheme in conjunction with a magnetic structure which absorbs the instantaneous voltage differences among cells. Stated another way, the individual cells should be made to behave as current sources for times on the order of the switching period.

The interphase transformer (IPT) is the standard structure for paralleling two converters [3,7-8], and can be extended to more converter cells using many legged IPTs [9] or wiffle tree connections of IPTs [10]. However, these designs are inappropriate for paralleling large numbers of cells, because they are difficult to manufacture, and the cells cannot be made autonomous (an important condition for increased system reliability). Another approach is to place an inductor at the output of each bridge leg [4,11-12]. This structure results in a converter system which is modular and more easily manufactured. However, the size of the output inductor is an important design issue, since it can represent an appreciable fraction of converter size and cost. Minimization of the energy storage requirement of the output inductor is thus a key design goal for a practical parallel architecture.

SIZING OF BRIDGE OUTPUT INDUCTANCE

Consider the single-phase half-bridge converter of Fig. 1 operating under hysteretic current control. The converter drives a constant output voltage representing the output filter, the load, and other paralleled cells for times on the order of the switching period. Given a maximum switching frequency f_{sw}, a reference current i_{ref}, and a specified hysteresis band

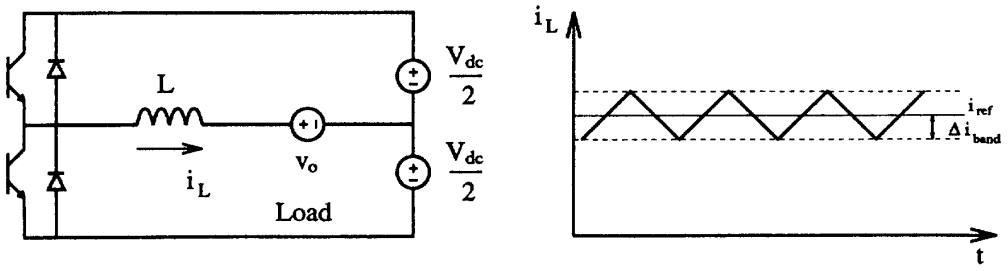

Fig. 1 The half-bridge current-controlled inverter and its output current waveform.

Δi_{band}, the energy storage requirement of the inductor is:

$$W_t = \frac{i_{ref} V_{dc}}{16 f_{sw}} \frac{(1+k)^2}{k} \qquad (1)$$

where $k = \Delta i_{band}/i_{ref}$. Figure 2 shows a plot of (1) as a function of k, and shows that the minimum of this curve occurs at $k = 1$, with only minor increases in energy storage for values over 1. At $k = 1$, the ripple band has the same magnitude as the reference current. If a purely capacitive snubber is placed across each device, operation at $k = 1$ yields a circuit with zero-voltage turn off and zero current turn on of the main devices. In situations where the devices have very fast turn-off and high conduction loss penalties (such as MOSFETS), this operating principle may be the most desirable. However, it is also desirable to remove the turn-on losses due to capacitor dump that occur with this operating mode. As we show in the next section, placing a capacitive snubber across each device and increasing k to a value slightly over 1 yields a cell topology with zero-voltage switching at both turn on and off, and zero-current turn on. This is achieved at small additional cost in inductor energy storage requirements.

THE RESONANT POLE INVERTER

The converter topology shown in Fig. 3, originally presented in [13], is known as the resonant pole inverter (RPI) [14]. The operation of this converter is illustrated in Fig. 4 and described as follows: Suppose operation begins with S_1 conducting (mode 1). Assuming that the filter capacitor is large enough to clamp the output voltage over the cycle, the inductor current will build up linearly until it reaches a current i_{p+} determined by the controller. At this point, the controller turns S_1 off at zero voltage, and the inductor rings with the two resonant capacitors (mode 2) until D_2 turns on (mode 3). The switch S_2 is then turned on at

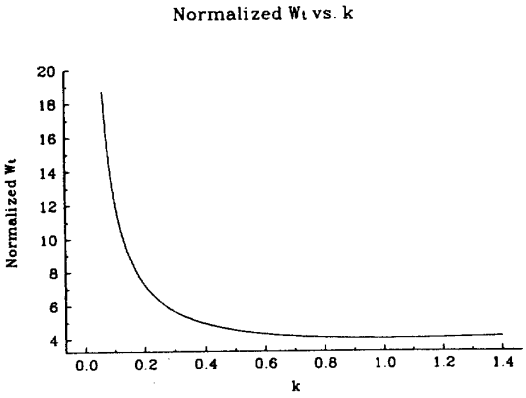

Fig. 2 Output inductor energy storage requirement as a function of ripple ratio, k.

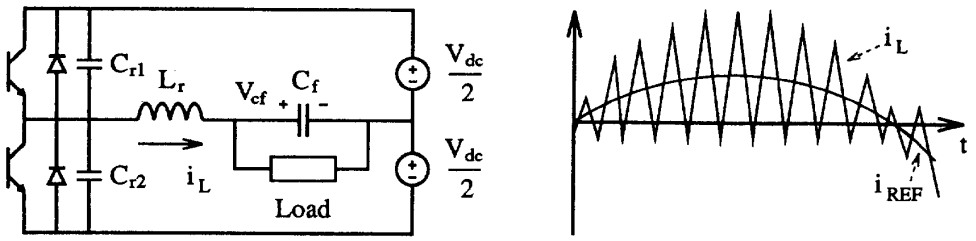

Fig. 3 The resonant pole inverter and its output current waveform.

zero voltage while D_2 conducts. During this time, the current in the inductor linearly decreases and reverses direction (mode 4). When the reverse current in the inductor reaches a level i_{p-}, the controller turns off S_2 at zero voltage, and the inductor rings with the resonant capacitors (mode 5) until D_1 conducts (mode 6). The switch S_1 can then be turned on at zero voltage, and the cycle repeats.

As with standard hysteresis-based PWM, the switching frequency varies dynamically. If the length of the resonant transitions are small and do not affect the inductor current heavily, the instantaneous switching period can be approximated as:

$$T \approx \frac{V_{dc} L_r (i_{p+} + i_{p-})}{\frac{1}{4} V_{dc}^2 - V_{cf}^2} \qquad (2)$$

Also, while the *peak* current stresses are somewhat high compared to a hard-switched converter (~2-2.5 p.u.), the rms current stresses are much lower (~1.1-1.4 p.u.). For many power devices, this represents only a small cost penalty.

The values of i_{p+} and i_{p-} used by the controller are constrained by the necessity of having enough energy in the inductor to ring the resonant capacitor voltages to zero for

Tables 1,2 RPI control tables

i_{ref}	< 0	> 0
	$i_{p+} = i_z$ $i_{p-} = 2i_{ref} - i_z$ $i_z = i_m$	$i_{p+} = 2i_{ref} + i_z$ $i_{p-} = -i_z$ $i_z = i_m$

Table 1

i_{ref} / V_{cf}	< 0	> 0
> 0	$i_{p+} = i_z$ $i_{p-} = 2i_{ref} - i_z$ $i_z = i_m$	$i_{p+} = 2i_{ref} + i_z$ $i_{p-} = -i_z$ $i_z = \max(i_m - 2i_{ref}, 0)$
< 0	$i_{p+} = i_z$ $i_{p-} = 2i_{ref} - i_z$ $i_z = \max(i_m + 2i_{ref}, 0)$	$i_{p+} = 2i_{ref} + i_z$ $i_{p-} = -i_z$ $i_z = i_m$

Table 2

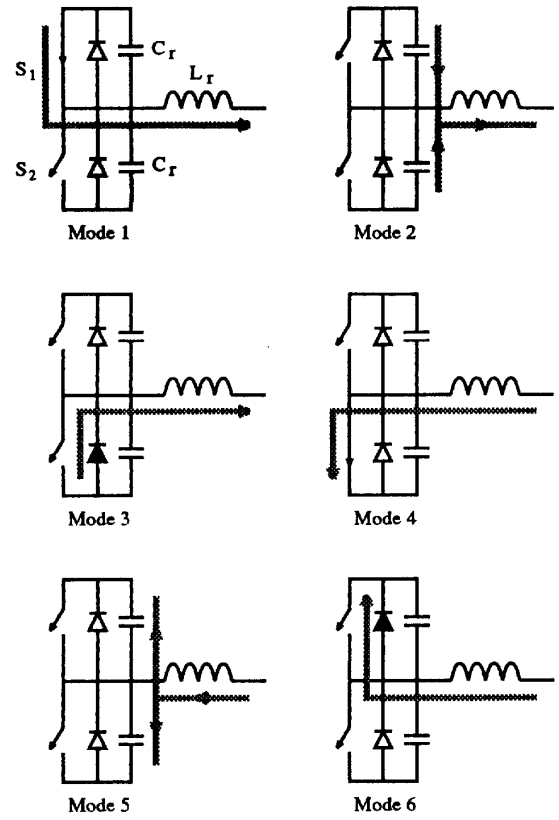

Fig. 4 An operational cycle of the resonant pole inverter.

zero-voltage switching. Assuming ideal components, a minimum inductor current i_{min} is needed at the end of mode 1 if $V_{cf} > 0$, where we define:

$$i_{min}(V_{cf}) = 2\sqrt{\frac{C_r V_{dc} |V_{cf}|}{L_r}} \qquad (3)$$

No current is required for $V_{cf} \leq 0$. Similarly, the magnitude of i_{p-} must exceed i_{min} at the end of mode 4 if $V_{cf} < 0$, and may be zero for $V_{cf} \geq 0$.

Conventional RPI Control

A desired average output current i_{REF} is generated by controlling the values of i_{p+} and i_{p-}. If the time spent in the resonant transitions is small and does not severely affect the inductor current, the output current waveform can be treated as triangular, yielding an approximate average output current of $(i_{p+} + i_{p-})/2$. The conventional control method for generating a desired i_{REF} is shown in Table 1, where i_m is a current sufficiently greater than i_{min} to ensure reliable operation.

Enhanced RPI Control

While the conventional control approach is simple and always ensures that the resonant inductor current constraints are met, for many operating conditions it yields currents which are significantly higher than needed to ensure zero-voltage switching. Here we introduce a new control method, shown in Table 2, which reduces peak currents and losses for many operating conditions, and yields similar performance for all others. The new control method takes advantage of the fact that for a given output voltage polarity, there is a minimum inductor current requirement for only one of the two resonant transitions. When $V_{cf} > 0$, there is only a minimum required value for i_{p+}, and when $V_{cf} < 0$ there is only a minimum value for the magnitude of i_{p-}. Thus, when we are sourcing power from the converter (quadrants 1,3), we need only make up for any difference between the peak current needed to source i_{REF} alone and that required for the resonant transition. In quadrants 2 and 4, we are left with the conventional control method. The control method shown in Table 2 achieves this, and is simple to implement in analog hardware.

To see the benefits of this enhanced control technique, consider the simulation example illustrated in Fig. 5. The half bridge converter in this example is used to drive an *R-L* load at 65 volts and 60 Hz. For both control methods, the system has an outer PI voltage control loop, and uses a value of $i_m = i_{min}(V_{cf})$ with an additional constant safety margin for peak current calculations. The resonant inductor current is significantly reduced for the enhanced method, as are the device and filter capacitor currents. For the example shown, the rms filter capacitor current was reduced by over 15% compared to the conventional method. This benefit of the enhanced control algorithm is especially significant for converters which operate at partial load, since it improves partial-load efficiency by reducing the fixed losses associated with maintaining zero-voltage switching.

One minor disadvantage of the enhanced control method is that the approximate relationship among i_{REF}, i_{p+}, and i_{p-} is less accurate for the enhanced method than for the conventional method. Because the currents are lower for the enhanced method, more time is spent in the resonant transitions, and the overall waveform shape is affected more by the transitions. However, these effects are easily compensated for by using feedforward or feedback, and do not pose a significant problem, as can be seen by the

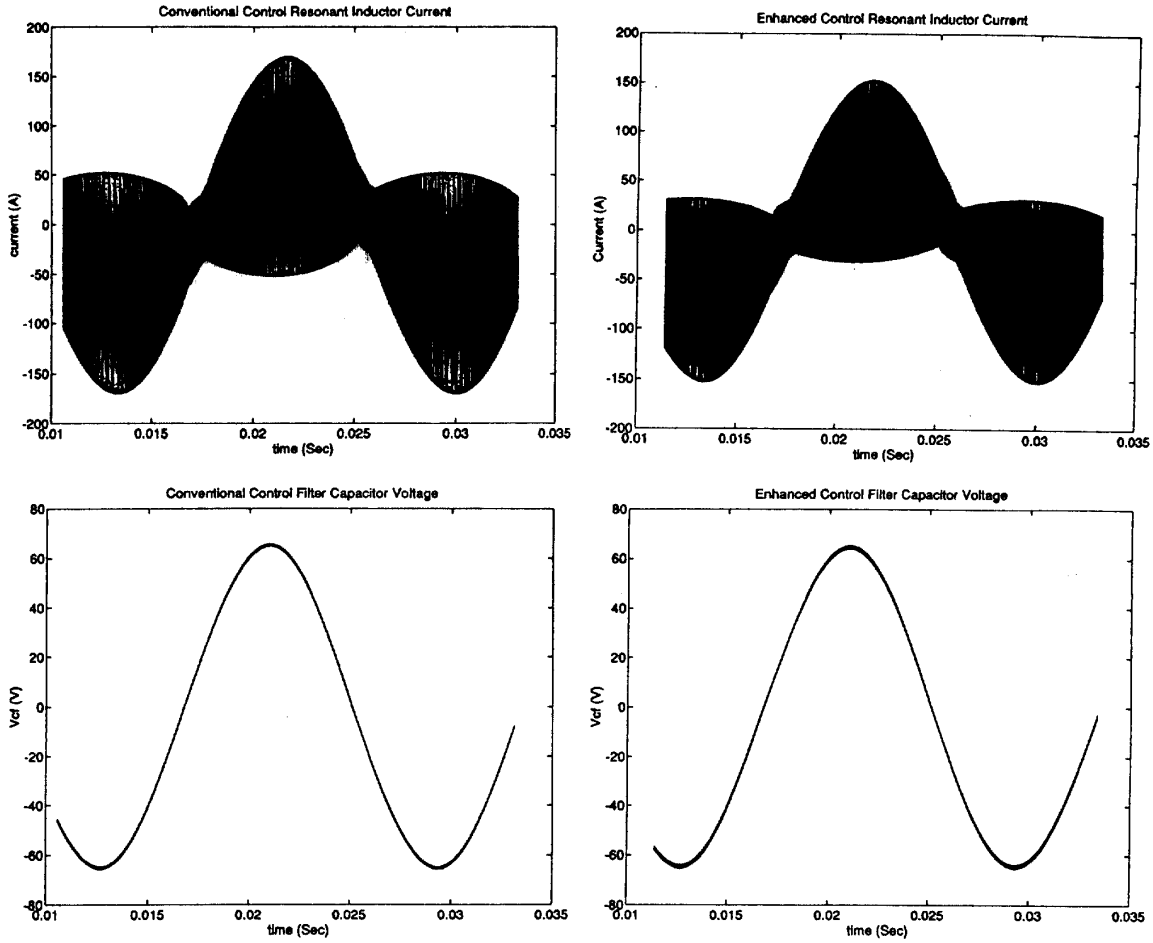

Fig. 5 Comparison of RPI control methods. RPI has $L_r = 15\ \mu H$, $C_r = 0.16\ \mu F$, $C_f = 150\ \mu F$, $L_l = 1$ mH, $R_l = 1\Omega$, $V_{dc} = 300$ V.

resulting waveform quality in Fig. 5.

THE PARALLEL RESONANT POLE INVERTER

An important contribution of this paper is the development of the *parallel* resonant pole inverter (PRPI) architecture shown in Fig. 6, which is based on the resonant pole structure. For simplicity, the single-phase half-bridge will be discussed here, although a three-phase circuit with equivalent properties can be formed. Constructing a parallel system using resonant pole inverter cells meets the objective of minimizing the size of the magnetic structure, since the RPI cells operate near the minimum energy storage point of (1). Furthermore, because this converter is fully soft-switched, it can operate at higher frequencies than a comparable hard-switched converter for the same total losses. As can be seen from (1), this increase in permissible operating frequency further reduces the size of the required magnetic components. These advantages are achieved with a minimum of added components and a simple control system.

Modeling of the PRPI

We now develop a piecewise model for simulating the general N-converter parallel resonant pole inverter (PRPI) system of Fig. 6. The model assumes ideal switches and

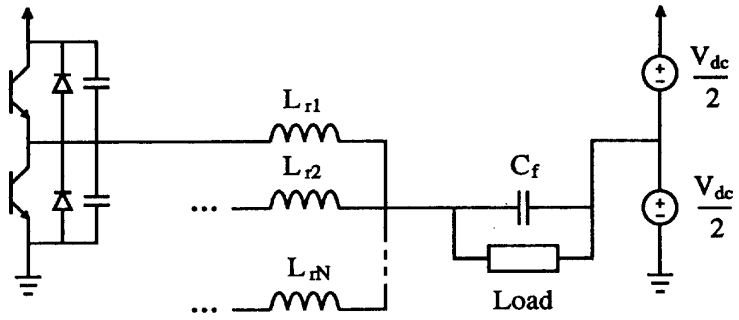

Fig. 6 The parallel resonant pole inverter architecture.

components, and an *R-L-E* load. State equations are given for the resonant inductor current and capacitor voltage of the i^{th} converter cell in each mode, along with boundary conditions for transition to the next mode. State equations valid under all conditions are presented for the filter capacitor voltage and load current.

The resonant inductor current and bottom resonant capacitor voltage for the k^{th} converter cell are denoted as i_{lk} and v_{c2k}, respectively. The voltage of the top resonant capacitor is entirely determined by the voltage across the bottom capacitor, and is thus not considered.

The state equations for the filter capacitor voltage and load current are as follows:

$$\frac{dV_{cf}}{dt} = \frac{(\sum_{k=1}^{N} i_{lk}) - i_{load}}{C_f} \tag{4}$$

$$\frac{di_{load}}{dt} = \frac{V_{cf} - i_{load}R_{load} - E_{load}}{L_{load}} \tag{5}$$

For the k^{th} cell in mode 1 or 6 (S_1/D_1 on, S_2/D_2 off):

$$\frac{di_{lk}}{dt} = \frac{\frac{1}{2}V_{dc} - V_{cf}}{L_{rk}} \tag{6}$$

$$\frac{dV_{c2k}}{dt} = 0. \tag{7}$$

This mode is valid until the inductor current reaches the specified value and S_1 is turned off.

For the k_{th} cell in mode 2 (S_1/D_1 off, S_2/D_2 off, top to bottom transition):

$$\frac{dV_{c2k}}{dt} = -\frac{i_{lk}}{2C_{rk}} \tag{8}$$

$$\frac{di_{lk}}{dt} = \frac{V_{c2k} - \frac{1}{2}V_{dc} - V_{cf}}{L_{rk}} \tag{9}$$

This mode is valid while $V_{c2k} > 0$.

For the k^{th} cell in mode 3 or 4 (S_1/D_1 off, S_2/D_2 on):

$$\frac{di_{lk}}{dt} = \frac{-\frac{1}{2}V_{dc} - V_{cf}}{L_{rk}} \tag{10}$$

$$\frac{dV_{c2k}}{dt} = 0. \tag{11}$$

This mode is valid until the inductor current reaches the specified value and S_2 is turned off.

For the k_{th} cell in mode 5 (S_1/D_1 off, S_2/D_2 off, bottom to top transition):

$$\frac{dV_{c2k}}{dt} = -\frac{i_{lk}}{2C_{rk}} \tag{12}$$

$$\frac{di_{lk}}{dt} = \frac{V_{c2k} - \frac{1}{2}V_{dc} - V_{cf}}{L_{rk}} \tag{13}$$

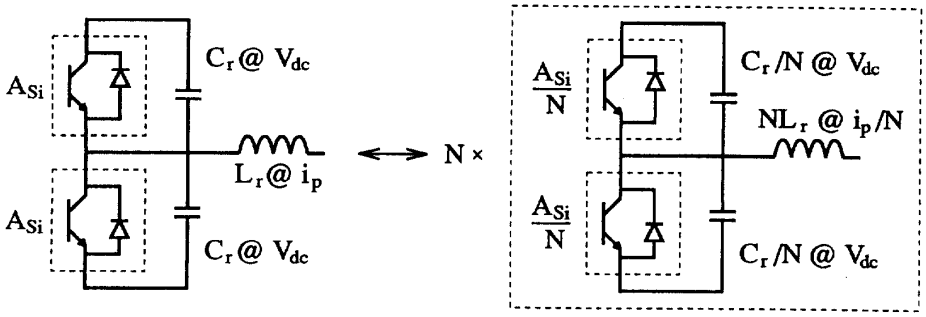

Fig. 7 A resonant pole inverter leg and its equivalent parallel resonant pole components

This mode is valid while $V_{c2k} < V_{dc}$.

The relevant state equations are solved at each time step, changing the modes of the individual converters as necessary. This method is used for the simulation results presented in this paper.

Advantages of the PRPI

In addition to its other attributes, such as simplicity, high-frequency operation, ease of control, and minimal output magnetics, the PRPI eliminates two of the major drawbacks of the conventional RPI. As discussed in [15], the practical size of an RPI is limited by the difficulty of constructing output inductors of large enough rating with off-the-shelf components. However, an N cell PRPI can be constructed which is functionally equivalent to a single RPI of N times the cell VA rating, increasing the converter size by a factor of N over that achievable using a single RPI. To see this, consider breaking down a single RPI into N cells as shown in Fig. 7. Each of these converter cells will, to first order, operate at the same frequency as the original, and have $1/N$ times the losses. Thus, creating the same VA rating with equivalent parallel cells distributes the inductance in a manner which makes it far more manufacturable than a single large converter. This benefit is in addition to the fact that in practice, the smaller converters can be designed to operate at higher frequencies than a single large converter, due to the availability of higher-performance devices, reduction of parasitics and the distribution of heat generation [2].

Another serious difficulty with resonant pole inverters is the high current ratings of the output filter capacitors [16]. As we will show, ripple cancellation among the individual converters of a PRPI significantly reduces the rms current stress on the filter capacitors, even under independent open loop control of the individual cells.

Consider the relative performances of a single RPI and a 10 cell PRPI, both operating under the conventional control method with fixed i_m, as shown in Fig. 8. The rms current stresses on the filter capacitor are reduced by over 70% in the PRPI as compared to the single equivalent RPI, and the voltage ripple is lower as well. This reduction is due to the lack of coherence among the aggregated outputs of the cells, and is likely to be useful for diminishing acoustic noise and EMI as well. Interdependent control of the PRPI converters, or locally-controlled ripple cancellation schemes would further improve the advantage of the PRPI. Thus, the use of a parallel scheme significantly reduces the requirements on the output filter, even when the converters are controlled autonomously.

CONCLUSION

We have described a parallel converter architecture based on the resonant pole topology, and shown that the architecture meets the important objective of minimizing the required output magnetics, while retaining the simplicity of the basic bridge structure. We have also introduced a novel current control scheme applicable to both the new parallel architecture and the single resonant pole inverter. This control scheme significantly reduces converter losses and stresses under many operating conditions compared to the conventional control method. Equations for piecewise

modeling of the new architecture are also presented. Finally, the paper demonstrates that the PRPI architecture overcomes some of the major disadvantages of the single RPI.

REFERENCES

[1] J. Kassakian, "High Frequency Switching and Distributed Conversion in Power Electronic Systems", *Sixth Conference on Power Electronics and Motion Control (PEMC 90)*, Budapest, 1990.

[2] J. Kassakian and D. Perreault, "An Assessment of Cellular Architectures for Large Converter Systems", *First International Conference on Power Electronics and Motion Control (IPEMC 94)*, Beijing, June 1994, (in press).

[3] M. Honbu, Y. Matsuda, K. Miyazaki, and Y. Jifuku, "Parallel Operation Techniques of GTO Inverter Sets for Large AC Motor Drives", *IEEE IAS Annual Meeting*, 1982, pp. 657-662.

[4] M. Hashii, K. Kousaka, and M. Kaimoto, "New Approach to a High Power GTO PWM Inverter for AC Motor Drives", *IEEE IAS Annual Meeting*, 1985, pp.467-472.

[5] S. Tadakuma, S. Tanaka, K. Miura, H. Inokuchi, and H. Ikeda, "Fundamental Approaches to PWM Control Based GTO Inverters for Linear Synchronous Motor Drives", *IEEE IAS Annual Meeting*, 1991, pp. 847-853.

[6] J. Holtz, W. Lotzkat, and K. Werner, "A High-Power Multitransistor-Inverter Uninterruptible Power Supply System", *IEEE Transactions on Power Electronics*, Vol. 3, No. 3, July 1988, pp. 278-285.

[7] S. Okuma, K. Iwata, and K. Suzuki, "Parallel Running of GTO PWM Inverters", *IEEE Power Electronics Specialists Conference Record*, 1984, pp. 111-120.

[8] S. Ogasawara, J. Takagaki, H. Akagi, and A. Nabae, "A Novel Control Scheme of a Parallel Current-Controlled PWM Inverter", *IEEE Transactions on Industry Applications*, Vol. 28, No. 5, Sept/Oct 1992, pp. 1023-1030.

[9] J. Schaefer, Rectifier Circuits: Theory and Design, John Wiley and Sons, NY, NY, 1965, pp. 49-51.

[10] K. Matsui, "A Pulsewidth Modulated Inverter with Parallel-Connected Transistors Using Current Sharing Reactors", *IEEE Transactions on Power Electronics*, Vol. 8, No. 2, April 1993, pp. 186-191.

[11] M. Youn and R. Hoft, "Analysis of Parallel Operation of Inverters", *IEEE IAS Annual Meeting*, 1976, pp. 951-958.

[12] F. Petruzziello, P. Ziogas, and G. Joos, "A Novel Approach to Paralleling of Power Converter Units with True Redundancy" *IEEE Power Electronics Specialists Conference Record*, 1990, pp. 808-813.

[13] D. Divan and G. Skibinski, "Zero Switching Loss Inverters for High Power Applications, *IEEE IAS Annual Meeting*, 1987, pp. 627-634.

[14] R. DeDoncker, D. Divan, and T. Lipo, "High Power Soft Switching Inverters", *PESC '91 Tutorial*, 1991.

[15] B. Acharya, R. Gascoigne, and D. Divan, "Active Power Filters Using Resonant Pole Inverters", *IEEE IAS Annual Meeting*, 1989, pp.967-973.

[16] D. Divan and G. Venkataramanan, "Comparative Evaluation of Soft Switching Inverter Topologies", *1991 European Power Electronics Conference (EPE)*, 1991, pp. 2-013 - 2-018.

[17] J.G. Cho, D.Y. Hu, and G.H. Cho, "Three Phase Sine Wave Voltage Source Inverter Using the Soft Switched Resonant Poles", *IEEE Industrial Electronics Conference (IECON)*, 1989, pp. 48-53.

[18] D. Divan, G. Venkataramanan, and R. DeDoncker, "Design Methodologies for Soft Switched Inverters", *IEEE Transactions on Industry Applications*, Jan/Feb 1993, pp 126-135.

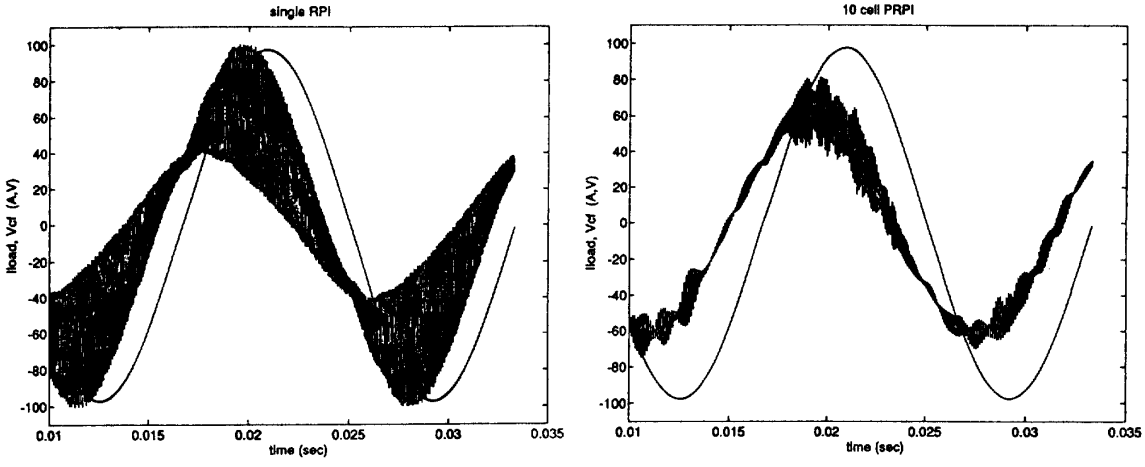

Fig. 8 Comparison of an RPI and equivalent PRPI. RPI has $L_r = 25\ \mu H$, $C_r = 0.16\ \mu F$, $C_f = 50\ \mu F$, $L_l = 1$ mH, $R_l = 0.5\Omega$, $V_{dc} = 300$ V.